Needle force sensor for improved accuracy during prostate biopsies through the differentiation of tissue

Timothy Tarnopolsky[1,3], Rachel Hoki[2,3], Mariana Bernardes[3], Pedro Moreira[3], Junichi Tokuda[3]

McNair Academic High School, 123 Coles St, Jersey City, NJ 07302[1], Liberty High School, 16655 SE 136th St, Renton, WA 98059[2], Brigham and Women's Hospital, 75 Francis St, Boston, MA 02115[3]

Introduction

Prostate cancer is the second most common form of cancer found in men. A prostate biopsy is done to collect small tissue samples when the prostate-specific antigen level in a person's blood is elevated, or when an abnormality is found during a person's digital rectal exam. Trials[1-2] suggest that magnetic resonance imaging (MRI) is preeminent in prostate biopsies due to its ability to differentiate between diseased and normal tissue accurately. However, recent studies suggest that MRI-guided prostate biopsies suffer from inaccuracy due to stiff anatomical structures, such as the pelvic diaphragm, which causes major deflections[3-4]. In-vivo force measurement is crucial for differentiating stiff structures and potentially improving the needle placement accuracy. We developed and validated an attachable needle force sensor that is MRI-compatible (ANFS-M) to achieve this goal.

Methods

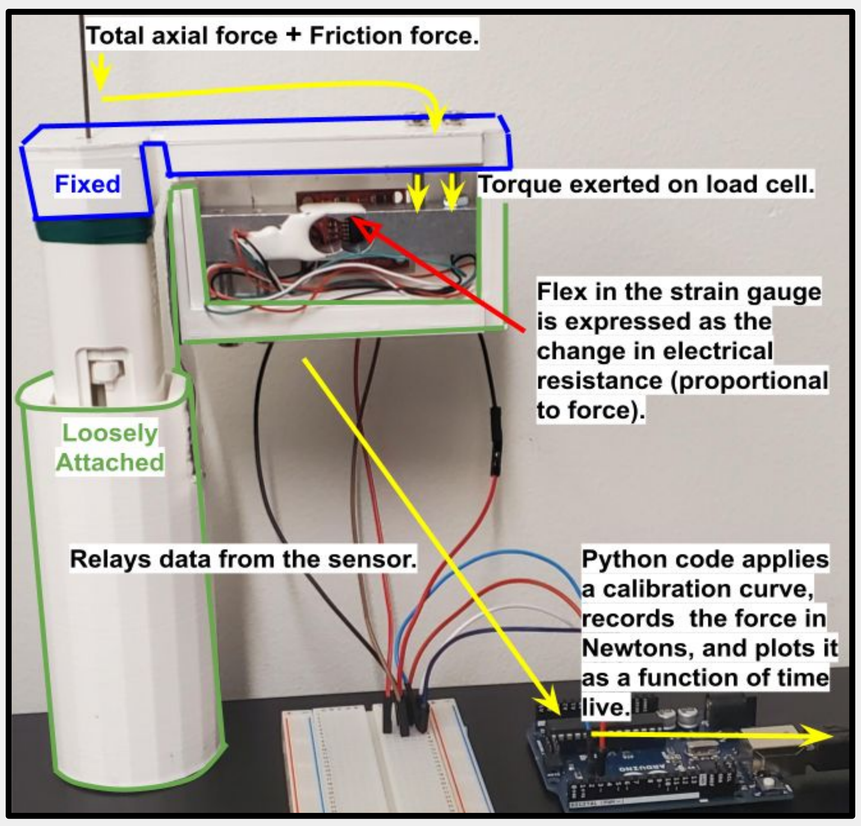

Fig. 1. Design and force distribution of the ANFS-M

Validation: Our working hypothesis is that the ANFS-M can differentiate tissues with different stiffnesses. The ANFS-M was used in needle insertions into three homogeneous phantoms made from different concentrations of agar (0.0291/15g, 0.0385/20g, and 0.0483/25g) labeled accordingly as 15g, 20g, and 25g. Prior to experimentation the load cell was calibrated through the use of known masses. The displacement of the needle tip was recorded using an optical 3D tracking system (Polaris Vicra, Northern Digital Inc.). We used the force data collected by the ANFS-M, along with the displacement and velocity to model the total axial force and friction force exerted on the tip of the needle.

Results

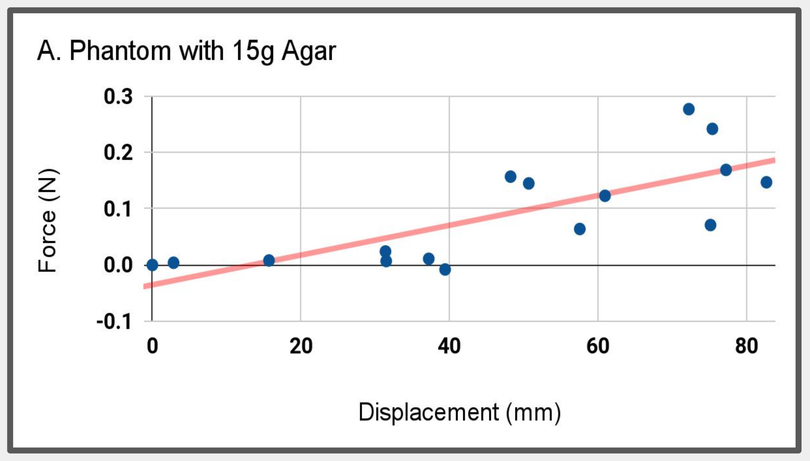

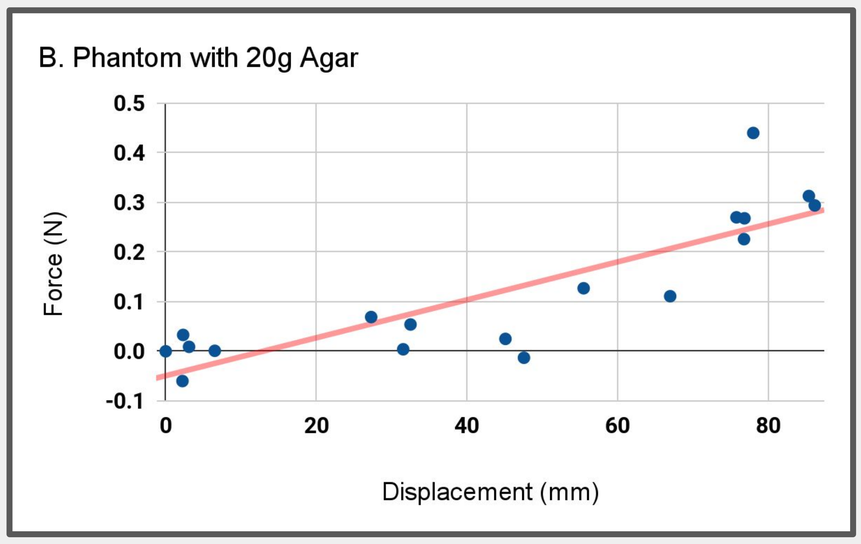

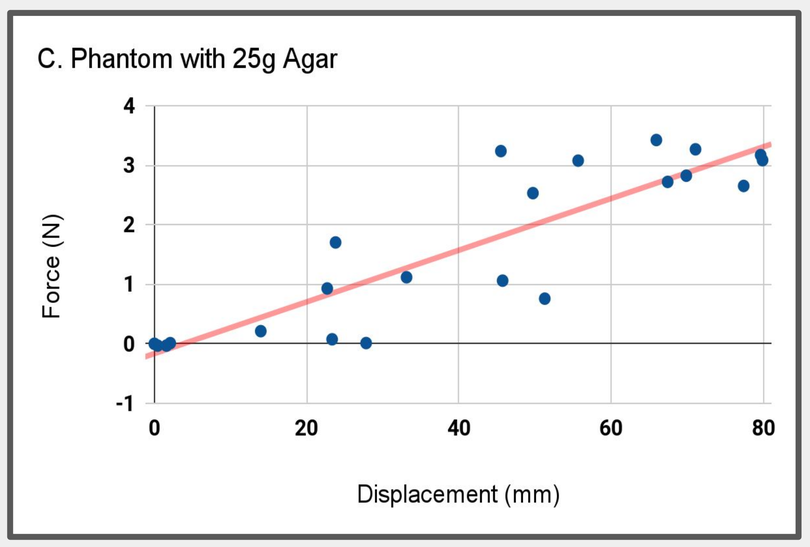

Fig. 2. Total axial force and friction force exerted on the tip of the needle during insertion into multiple homogeneous phantoms as a function of the needle tips displacement. The fitted straight line for:

A. is $y = (2.65 * 10^{-3})x - 0.0353$

B. is $y = (3.82*10^{-3})x - 0.0492$

C. is $y = 0.0434x - 0.165$

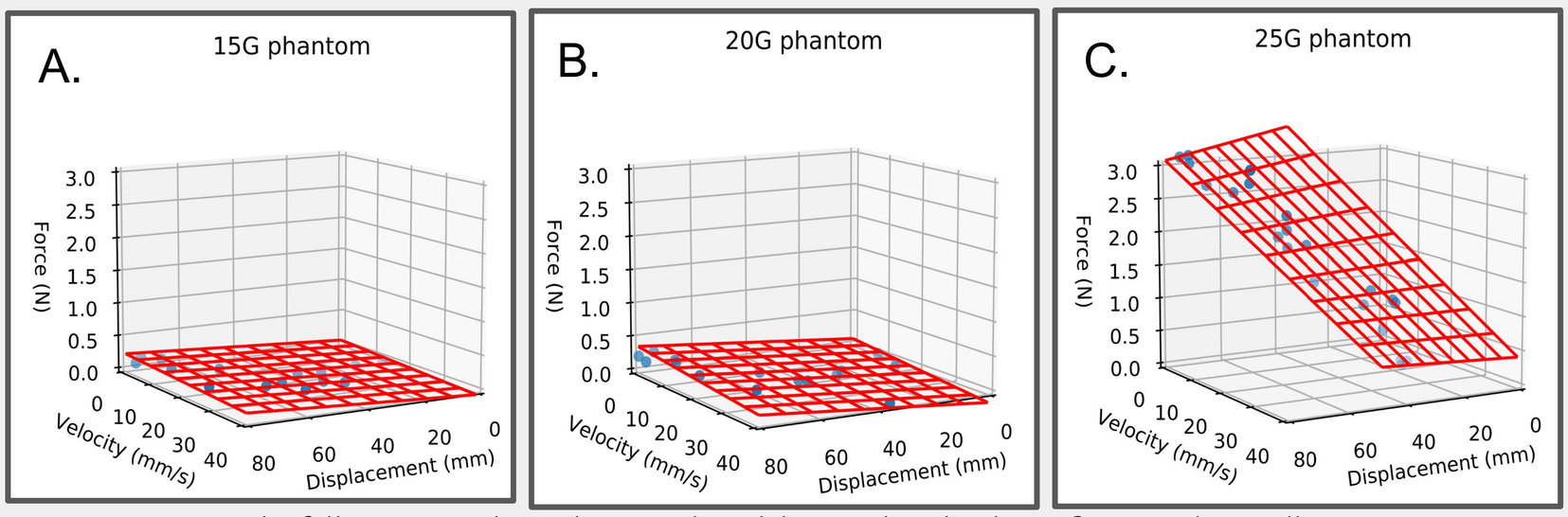

Fig. 3. We assume the following simple mathematical model to predict the thrust force on the needle:

$$F = aD + bv + c$$

where is the force (N), is the displacement of the needle tip from the entry point (mm), and is the velocity of the needle tip (mm/s). and are the weighting factors for the displacement and the velocity respectively, whereas c is the offset.

Discussion

During the phantom punctures the displacement of the needle tip was found to be proportional to the force, as the deeper the needle entered in the phantom the more friction it faced. Additionally, the force also depends on the velocity of the needle tip, though the relationship varies based on the stiffness of the phantom. In Fig. 3. A. & B. the pliability of the phantoms along with human instinct to reduce speed when meet with a force caused velocity to be low when the force was high. In Fig. 3. C. the greater stiffness allowed for more uniform velocities. Still, the ANFS-M differentiated the stiffness of the phantoms as evident by the steeper slopes for the phantoms made with higher concentrations of agar present in Fig. 2 & 3 (**15g → 2.65 * 10^{-3} < 20g → 3.82*10^{-3} < 25g → 0.0434**).

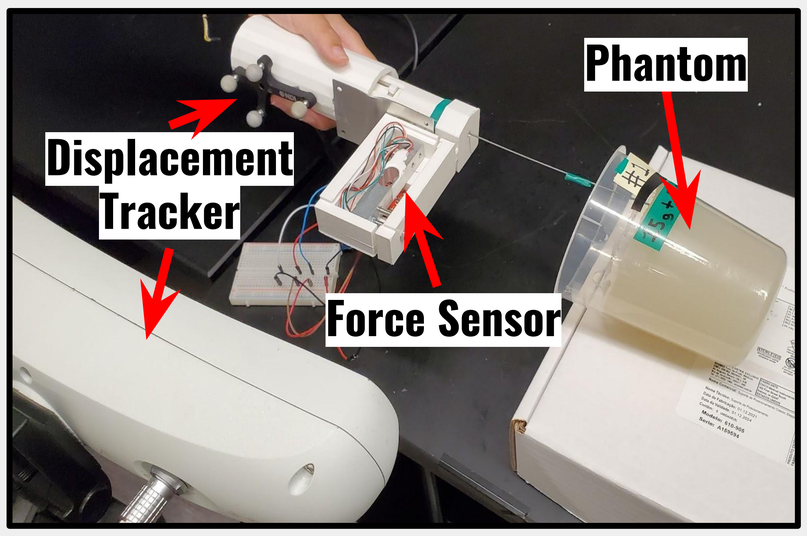

References

1. Kasivisvanathan V, Rannikko AS, Borghi M, Panebianco V, Mynderse LA, Vaarala MH, Briganti A, Budäus L, Hellawell G, Hindley RG, Roobol MJ, Eggener S, Ghei M, Villers A, Bladou F, Villeirs GM, Virdi J, Boxler S, Robert G, Singh PB, Venderink W, Hadaschik BA, Ruffion A, Hu JC, Margolis D, Crouzet S, Klotz L, Taneja SS, Pinto P, Gill I, Allen C, Giganti F, Freeman A, Morris S, Punwani S, Williams NR, Brew-Graves C, Deeks J, Takwoingi Y, Emberton M, Moore CM; PRECISION Study Group Collaborators. MRI-Targeted or Standard Biopsy for Prostate-Cancer Diagnosis. N Engl J Med. 2018 May 10;378(19):1767-1777. doi: 10.1056/NEJMoa1801993. Epub 2018 Mar 18. PMID: 29552975; PMCID: PMC9084630.
2. Bjurlin MA, Mendhiratta N, Wysock JS, Taneja SS. Multiparametric MRI and targeted prostate biopsy: Improvements in cancer detection, localization, and risk assessment. Cent European J Urol. 2016;69(1):9-18. doi: 10.5173/ceju.2016.734. Epub 2016 Jan 25. PMID: 27123316; PMCID: PMC4846729.
3. Moreira P, Patel N, Wartenberg M, Li G, Tuncali K, Heffter T, Burdette EC, Iordachita I, Fischer GS, Hata N, Tempany CM, Tokuda J. Evaluation of robot-assisted MRI-guided prostate biopsy: needle path analysis during clinical trials. Phys Med Biol. 2018 Oct 16;63(20):20NT02. doi: 10.1088/1361-6560/aae214. PMID: 30226214; PMCID: PMC6198326.
4. Moreira P, Grimble J, Iftimia N, Bay CP, Tuncali K, Park J, Tokuda J. In vivo evaluation of angulated needle-guide template for MRI-guided transperineal prostate biopsy. Med Phys. 2021 May;48(5):2553-2565. doi: 10.1002/mp.14816. Epub 2021 Mar 24. PMID: 33651407; PMCID: PMC8141017

Acknowledgments

Thank you Junichi, Mariana, and Pedro for working with me throughout RISE and making it a great 6 weeks.

This study is supported in part by the National Institutes of Health (R01EB020667).